JOURNAL OF MATERIALS SCIENCE **39** (2004) 3057– 3061

Effect of grain size on elastic modulus and hardness of nanocrystalline ZrO_2-3 wt% Y_2O_3 ceramic

R. CHAIM
Department of Materials Engineering, Technion-Israel Institute of Technology, Haifa 32000, Israel

M. HEFETZ
Rafael, P.O. Box 2250, Haifa 31021, Israel

Dense nanocrystalline ZrO_2-3 wt% Y_2O_3 ceramics with grain sizes ranging between 23 to 130 nm were tested by ultrasonic pulse echo and Vickers hardness. The elastic modulus and hardness results were corrected for the residual porosity and the phase content. The corrected elastic moduli exhibited continuous decrease with decrease in the grain size. In contrast, no correlation was found between the corrected hardness and grain size. The percolative composite model was used to describe the changes in the elastic moduli in terms of percolation of the elastic wave through the intercrystalline phase at the percolation threshold. The absence of correlation with the hardness results was explained due to the other energy absorbing mechanisms such as microcracking beneath the indenter.

1. Introduction

Recently much effort has been invested in the characterization of the physical and mechanical properties of the nanocrystalline materials. The main difference between the bulk nanocrystalline materials and their conventional counterparts is the high density of the grain boundaries in the former, a fact that contributes to significant changes in the material properties. Due to the intrinsic brittleness of the ceramic crystals any reduction in their stiffness and yield strength may be important towards the gain of some ductility in their polycrystalline state. Superplasticity of Y_2O_3-stabilized tetragonal zirconia polycrystals (Y-TZP) is well documented in the literature [1]. The onset temperature for superplasticity was found to decrease with lowering the grain size [2, 3] in agreement with the phenomenological equation for superplasticity [4]. Nevertheless, this equation should take into account also any changes that occur in the elastic shear modulus and the yield strength due to the nanometer grain sizes. Moreover, in the light of the miniaturization of many different devices within which the grain size could be limited to the material component dimensions, it becomes important to determine the grain size effects on the mechanical properties of Y-TZP in the nanometer regime.

The present paper analyses the changes in the elastic modulus and hardness of nanocrystalline Y-TZP versus grain size, while considering the effects of porosity as well as the phase content on these properties.

2. Experimental procedure

Amorphous to nanocrystalline powders of ZrO_2-3 wt% Y_2O_3 (Y-TZP) were prepared by the sol-gel method, followed by cold pressing, presintering and hot isostatic pressing (HIP) to dense specimens. Fabrication conditions as well as the characterization parameters of these specimens have already been described in detail elsewhere [5]. Following the HIP process, dense cylindrical-shaped specimens, 11 mm in diameter and 10 mm in thickness were prepared. These specimens had the grain size in the range of 23 to 130 nm according to the X-ray line broadening measurements. In a few specimens, the grain size was also characterized by scanning and transmission electron microscopy (SEM/TEM) an example of which is shown in Fig. 1. The final densities ranged between 94 to 99% of the theoretical density as determined by the Archimedes method, while taking into account the phase content of each specimen.

The elastic modulus (E) was determined by the ultrasonic pulse-echo method, using a 10 mm diameter cylindrical transducer and longitudinal wave with the frequency of 2.25 MHz that was propagated along the specimens' axis. The accuracy in the wave travel time measurements was ± 1 μ·sec. The lengths of the specimens were determined within the accuracy of ± 2 μm.

Vickers pyramid hardness (VPH) tests were performed using a 500 g load for 10 s duration. Preliminary tests with increasing the load have shown the onset load for microcrack formation around the indent to be above

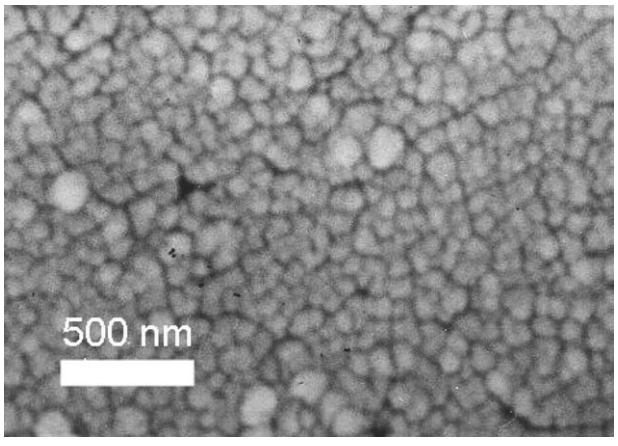

Figure 1 SEM image of the 97% dense hot-isostatically pressed nanocrystalline YTZP with average grain size of ~60 nm.

500 g. This load yields the average indentation size (diagonal) of 30 μm. Such indent size is larger by two orders of magnitude compared to the measured grain size and porosity (Fig. 1). Thus, the indented volume contains more than several thousands of nano-grains which is enough for measuring the specimens' bulk behavior. At least eight indentations were performed for determining the average hardness of each specimen.

The elastic modulus and hardness of a commercial (HIPed) fully dense fully-tetragonal Y-TZP (4 wt% Y_2O_3) as well as skull-melted polycrystalline monoclinic (pure) zirconia with average twin size of 1 μm were measured as the reference specimens.

3. Results

3.1. Elastic modulus

The overall results were summarized in Table I. The grain size versus final density showed that denser specimens were associated with finer grain size. This finding which is related to the presintering conditions was discussed in a previous paper [5]. However, the measured elastic moduli decreased with increase in the relative density (Fig. 2), in contrast to that expected for conventional materials. Nevertheless, the measured elastic moduli may be affected by porosity, phase assemblage and grain size. Once the actual values of the elastic moduli of the specimens together with their porosity and phase content were determined (Table I), the effects of the last two parameters on the first could be evaluated. In this respect, the elastic modulus of the porous specimen is expressed by [6]:

$$E = E_0 \cdot e^{(-bP)} \tag{1}$$

where E_0 is the elastic modulus of the fully dense material, P is volume fraction of the porosity and b is an empirical constant ranging between 2 to 4. The relatively low volume fraction of the porosity (below 6%) in the present specimens assures its closed nature, the effect of which on the elastic modulus is far smaller than open porosity. This in turn will enable us to use the simple approximation in Equation 1. Using the data for E in Table I and assuming $b = 2$ for Y_2O_3-stabilized zirconias [7], the elastic moduli of the present specimens in their fully dense conditions were calculated (E_0 values in Table I).

At this stage, one may consider the effect of the phase content on the elastic modulus, since the specimens contained different volume fractions of the tetragonal and monoclinic phases. A vast amount of data has been published on the elastic moduli of zirconia alloys and especially on their elastic constants [8–15]. These data, which cover a wide range of the Y_2O_3 compositions, indicate a relatively small difference between the elastic moduli of the cubic (*c*), tetragonal (*t*) and monoclinic (*m*) polymorphs of zirconia. This finding is not unexpected since the *t* and *m* crystal structures of zirconia resemble a slightly distorted version of the fluorite-type *c* crystal structure. These crystal structures also exhibit similar lattice parameters as well as densities [16]. The published elastic constants were used to calculate the elastic moduli with respect to the Hill's approach [17]. Thus, the most reproducible values for the elastic moduli of the *c*, *t*, and *m* phases in the Y_2O_3-stabilized zirconias were chosen as 220, 214 and 230 GPa, respectively.

In order to reveal the net effect of the grain size on the elastic modulus the E_0 values were normalized to exclude the phase content effects, as will be described below. The most exact solution for the elastic modulus of a multiphase system was derived by Hashin and Shtrikman [18]. However, similar results especially for phases of similar properties could be obtained through the Hill's model which represents the algebraic average of the values derived by Voigt and

TABLE I Characteristics of the nanocrystalline Y-TZP specimens

No.	Density (%)	Grain size (nm)	V_t^a (%)	E (GPa)	E_0 (GPa)	E_0^n (GPa)	H (GPa)	H_0 (GPa)	H_0^n (GPa)
1	99	23	42	178	182	171	10.97	11.76	7.96
2	99	35	31	198	202	188	9.26	9.93	6.24
3	96	43	31	195	211	186	9.24	12.22	6.23
4	97	45	33	210	223	210	9.08	11.20	6.21
5	97	58	17	250	265	250	10.29	12.69	6.26
6	95	82	31	246	272	246	9.11	12.93	6.14
7	94	106	32	236	266	236	7.22	10.99	4.90
8	94	107	58	246	277	246	8.82	13.42	7.07
9	94	130	34	246	277	246	8.72	13.27	6.00
10	100	500	97	307	307	306	14.21	14.21	14.00
11	100	1000	0	213	213	213	6.17	6.17	6.17

[a] $V_t + V_m = 1$.

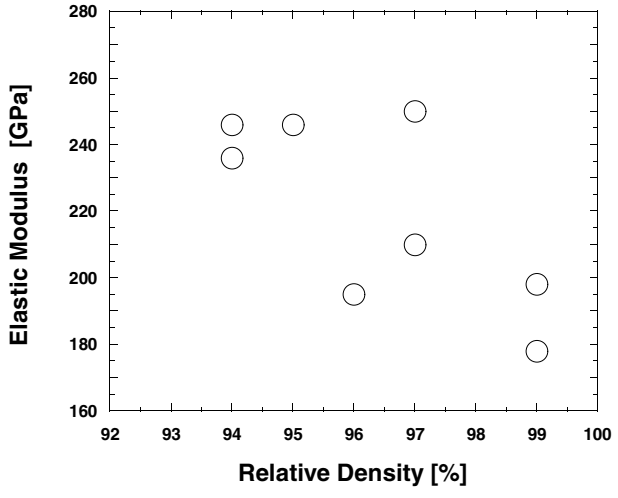

Figure 2 Measured elastic modulus versus final density of the nanocrystalline Y-TZP's.

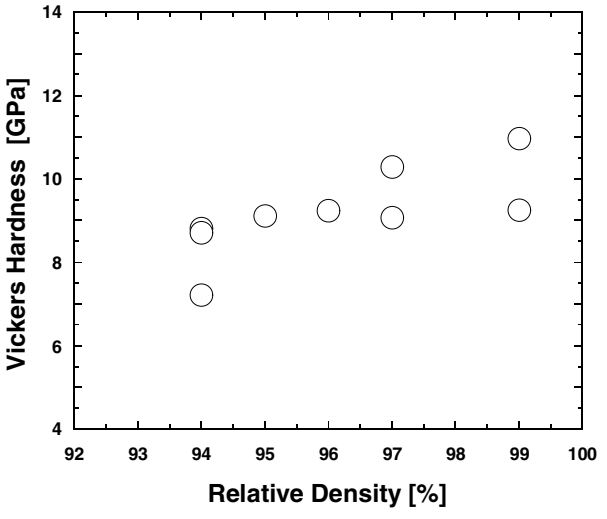

Figure 4 Measured Vicker hardness versus final density of the nanocrystalline Y-TZP's.

Reuss approximations [19]. These values were calculated according to the following equations:

$$E_V = V_t \cdot E_t + (1 - V_t) \cdot E_m \quad (2)$$

$$\frac{1}{E_R} = \frac{V_t}{E_t} + \frac{(1 - V_t)}{E_m} \quad (3)$$

$$E_H = \frac{E_V + E_R}{2} \quad (4)$$

where V_t is the volume fraction of the t phase, and the indices V, R, H, t, and m refer to Voigt, Reuss, Hill, tetragonal and monoclinic, respectively. Using the values of $E_t = 214$ GPa and $E_m = 230$ GPa, the previously calculated E_0 values were normalized (E_0^n in Table I) by multiplying it with the factor (E_t/E_H) with respect to V_t of each specimen. Therefore, the resultant elastic moduli values are expected to be affected only by the grain size. The values versus grain size were shown in Fig. 3 and exhibit a sharp decrease of the elastic modulus with decrease in grain size.

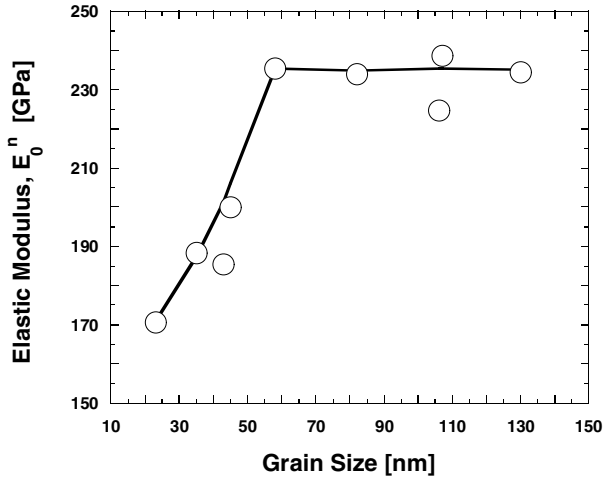

Figure 3 Elastic modulus values corrected for porosity and the phase content versus the grain size.

3.2. Hardness

The measured hardness was found to increase with density as shown in Fig. 4. A similar approach was used to analyze the hardness raw data in order to reveal the net effect of the grain size on hardness. In this respect, the hardness of the specimens in their fully dense condition may be calculated using the empirical expression developed for ceramics [20]:

$$H = H_0 \cdot e^{(-BP)} \quad (5)$$

where H_0 is the hardness of the fully dense ceramic, P is volume fraction of the porosity, and B is an empirical constant which was determined to be 7 for 4 wt% Y_2O_3-TZP [21]. These values were listed as H_0 in Table I. The hardness of the reference specimens were determined to be 14.21 and 6.17 GPa for the submicron grain size HIPed fully tetragonal (specimen #10) and the skull-melted polydomain monoclinic specimens (specimen #11), respectively.

In contrast to the similarities found in the elastic moduli of the zirconia polymorphs, their hardness was reported to be quite dissimilar [3, 22–26]. Considering the published hardness data for Y_2O_3-stabilized zirconias together with the results from the reference specimens, the values of 11.6 and 6.2 GPa were selected for the t and m phase, respectively. Again, considering the different volume fractions of the t and m phases in the specimens, the H_0 data were normalized in such a way that the hardness values became independent of the phase content. In this respect, the hardness of a homogeneous randomly distributed two-phase Y-TZP is given by the composites' hardness:

$$H_c = V_t \cdot H_t + (1 - V_t) \cdot H_m \quad (6)$$

where the index c refers to composite and the other characters have the same meanings as was mentioned earlier. Thus, using the hardness of the t and m phases together with V_t (Table I) and Equation 6, the composite hardness were determined. This was followed by multiplying the H_0 values by the normalizing factor

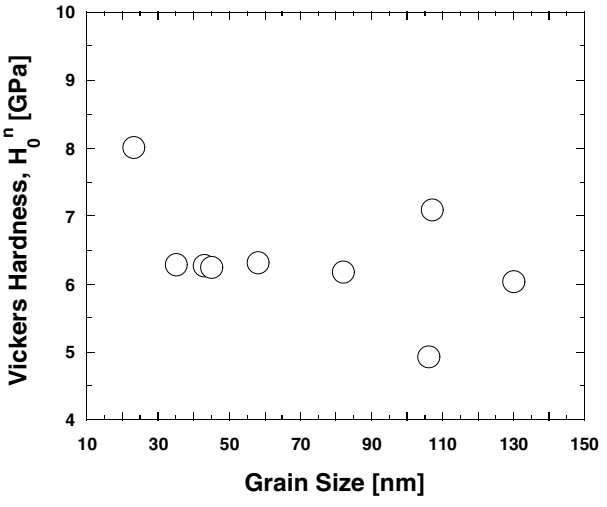

Figure 5 Vickers hardness values corrected for porosity and the phase content versus the grain size.

(H_c/H_t) which corresponded to the V_t of each specimen. The resultant values (H_0^n in Table I) which are independent of the phase content were plotted versus the grain size as shown in Fig. 5. In contrast to the elastic modulus, the hardness values had large scatter and no definite dependence on the grain size was found.

4. Discussion

Effects of the grain size on the mechanical properties such as the elastic modulus, yield strength and hardness were investigated mainly for nanocrystalline metals [27–34] and a few ceramics [35–37]. These investigations either support or negate the presence of such an effect on the mechanical properties. As a result, numerous models based on dislocations pile-up or composite approaches have been developed to explain the changes in hardness and yield strength at the nanometer regime. However, there is a general agreement that the elastic modulus decreases with grain size [27–29]. Such a decrease has been also shown by atomic embedded model and dynamic simulations [38–40]. In this respect, the nanocrystalline phase could be considered as a composite having grain boundary (intercrystalline) phase as well as grain interior (crystalline) phase. The mechanical and physical properties of the composite therefore depend on the corresponding properties of the composite constituents. However, such models have been unable to explain the significant and abrupt changes in the elastic modulus at the lower grain size range of the nanoscale regime [41, 42]. The percolative composite model [43] explained these changes in terms of the percolation of the elastic wave through the different intercrystalline microstructural components, i.e., grain-boundaries, triple-lines, and quadruple-nodes. These changes are expected to occur at the critical grain sizes at which the volume fractions of the intercrystalline components reach their threshold values needed for percolation. Deptuck *et al.* [44] measurements indicated a percolation threshold of 6.2% for elastic modulus of submicron-sized sintered silver powders. Using the threshold range of 6 to 15% for percolation of the elastic modulus together with the grain boundary thickness of 1 nm, the grain size range below which the percolation through the grain boundary 'phase' starts is about 28 to 60 nm [43] in agreement with the present results (Fig. 3). This finding supports the assumption about the lower elastic modulus contributed by the grain boundaries compared to that of the grain interiors.

In order to explain the difference between the elastic modulus and the hardness results with respect to their grain size dependencies, one should refer to the nature of these tests. While the ultrasonic pulse echo test is a nondestructive technique which samples the bulk of the material, the hardness test is destructive and samples only at the materials' surface. On the other hand, in order to reveal any effect of the grain size on the mechanical properties in the nanometer regime, the experimental results must be free of any artifacts (i.e., incorporation of other energy absorbing mechanisms). In this regard, the ultrasonic measurement is one of the most reliable techniques for determining the elastic properties. In contrast, hardness tests in ceramics are more complicated and often associated with both plastic deformation and microcracking. Different processes such as amorphisation, twinning and microcracking were observed by TEM beneath the hardness indentations and around them in nanocrystalline Y-TZP [45]. Thus the hardness measurements do not represent solely the relative contributions of the grain boundary and the grain interior strength, but also the energy absorbed due to other processes such as microcracking. Similar considerations hold for nanocrystalline ductile metallic alloys within which precipitation and second phase particles may contribute to hardening as well as induce microcracking during the hardness tests. These artifacts cause a large scatter in the hardness results as was found here and reported by others [46]. Consequently, characterization of the grain size effects in nanocrystalline materials is preferred by application of appropriate testing methods which allow nondestructive sampling of the materials' bulk structure.

Finally, the decrease in the elastic modulus with grain size may have significant effects on room temperature application as well as on superplastic deformation of nanocrystalline ceramics.

Acknowledgments

This research was supported by the E. and J. Bishop Research Fund at the Technion.

References

1. T. G. NIEH, J. WADSWORTH and F. WAKAI, *Inter. Mater. Rev.* **36** (1991) 146.
2. F. WAKAI and T. NAGANO, *J. Mater. Sci.* **26** (1991) 241.
3. G. B. PRABHU and D. L. BOURELL, *Scr. Metall. Mater.* **33** (1995) 761.
4. T. G. LANGDON, *Acta Metall. Mater.* **42** (1994) 2437.
5. R. CHAIM and M. HEFETZ, *J. Mater. Res.* **13** (1998) 1875.
6. R. M. SPRIGGS, *J. Amer. Ceram. Soc.* **45** (1962) 454.
7. A. J. A. WINNUBST, K. KEIZER and A. J. BURGGRAAF, *J. Mater. Sci.* **18** (1983) 1958.
8. C. F. SMITH and W. B. CRANDALL, *J. Amer. Ceram. Soc.* **47** (1964) 624.

9. N. G. PACE, G. A. SAUNDERS, Z. SUMENGEN and J. S. THORP, *J. Mater. Sci.* **4** (1969) 1106.
10. I. L. CHISTYI, I. L. FABELINSKII, V. F. KITAEVA, V. V. OSIKO, YU. V. PISAREVSKII, I. SIL'VESTROVA and N. N. SOBOLEV, *J. Raman Spect.* **6** (1977) 183.
11. R. P. INGEL, R. W. RICE and D. LEWIS, *J. Amer. Ceram. Soc.* **65** (1982) C-108.
12. H. M. KANDIL, J. D. GREINER and J. F. SMITH, *ibid.* **71** (1988) 265.
13. R. P. INGEL and D. LEWIS III, *ibid.* **71** (1988) 265.
14. M. V. NEVITT, S.-K. CHAN, J. Z. LIU, M. H. GRIMSDITCH and Y. FANG, *Physica* B **150** (1988) 230.
15. S.-K. CHAN, Y. FANG, M. GRIMSDITCH, Z. LI, M. V. NEVITT, W. M. ROBERTSON and E. S. ZOUBOULIS, *J. Amer. Ceram. Soc.* **74** (1991) 1742.
16. R. P. INGEL and D. LEWIS III, *ibid.* **69** (1986) 325.
17. R. HILL, *Proc. Phys. Soc. London, Sect.* A **65** (1952) 439.
18. Z. HASHIN and S. SHTRIKMAN, *J. Mech. Phys. Solids* **11** (1963) 123.
19. R. F. S. HEARMAN, "An Introduction to Applied Anisotropic Elasticity" (Oxford Univ. Press, Oxford, 1961) p. 27.
20. R. W. RICE, *Treatise Mater. Sci. Tech.* **2** (1977) 199.
21. *Idem.*, *Mater. Sci. Eng.* A **73** (1985) 215.
22. S. W. LEE, S. M. HSU and M. C. SHEN, *J. Amer. Ceram. Soc.* **76** (1993) 1937.
23. R. W. RICE, C. Cm. WU and F. BORCHELT, *ibid.* **77** (1994) 2539.
24. R. C. FIRST and A. H. HEUER, *ibid.* **75** (1992) 2302.
25. R. CHAIM, in "Mechanical Properties and Deformation Behavior of Materials with Ultra-fine Microstructures," edited by M. Nastasi, D. M. Parkin and H. Gleiter (Kluwer, Dordrecht, 1993) p. 547.
26. T. SAKUMA and M. SHIMADA, *J. Mater. Sci.* **20** (1985) 1178.
27. M. WALLER, J. DIEHL and H.-E. SCHAEFER, *Phil. Mag.* A **63** (1991) 527.
28. C. SURYANARAYANA, D. MUKHHOPADHYAY, S. N. PATANKER and F. H. FROES, *J. Mater. Res.* **7** (1992) 2114.
29. N. P. KOBELEV, YA. M. SOIFER, R. A. ANDRIEVSKI and B. GUNTHER, *Nanostr. Mater.* **2** (1993) 537.
30. J. LIAN, B. BAUDELET and A. A. NAZAROV, *Mater. Sci. Eng.* A **172** (1993) 23.
31. X. Y. QIN, X. R. ZHANG, G. S. CHENG and L. D. ZHANG, *Nanostr. Mater.* **10** (1998) 661.
32. S. SAKAI, H. TANIMOTO and H. MIZUBAYASHI, *Acta Mater.* **47** (1999) 211.
33. H. S. CAO, R. BONNET, J. J. HUNSINGER and O. ELKEDIM, *Scripta Mater.* **48** (2003) 531.
34. C.-W. NAN, X. LI, K. CAI and J. TONG, *J. Mater. Sci. Lett.* **17** (1998) 1917.
35. J. WANG, M. RAINFORTH and R. STEVENS, *Br. Ceram. Trans. J.* **88** (1989) 1.
36. K. LU, H. Y. ZHANG, Y. ZHONG and H. J. FECHT, *J. Mater. Res.* **12** (1997) 923.
37. A. BARVO-LEON, Y. MORIKAWA, M. KAWAHARA and M. J. MAYO, *Acta Mater.* **50** (2002) 4555.
38. D. CHEN, *Mater. Sci. Eng.* A **190** (1995) 193.
39. J. WANG, D. WOLF, S. R. PHILPOT and H. GLEITER, *Phil. Mag.* A **73** (1996) 517.
40. P. HEINO and E. RISTOLANINEN, *ibid.* **81** (2001) 957.
41. T. D. SHEN, C. C. KOCH, T. Y. TSUI and G. M. PHARR, *J. Mater. Res.* **10** (1995) 2892.
42. M. B. BUSH, *Mater. Sci. Eng.* A **161** (1993) 127.
43. R. CHAIM, *J. Mater. Res.* **12** (1997) 1828.
44. D. DEPTUCK, J. P. HARRISON and P. ZAWADZKI, *Phys. Rev. Lett.* **54** (1985) 913.
45. R. CHAIM, Unpublished work.
46. B. A. COTTOM and M. J. MAYO, *Scr. Mater.* **34** (1996) 809.

Received 5 June
and accepted 30 December 2003